sciendo

PRODUCTION ENGINEERING ARCHIVES 25 (2019) 60-65

PRODUCTION ENGINEERING ARCHIVES

ISSN 2353-5156 (print)
ISSN 2353-7779 (online)

Exist since 4th quarter 2013
Available online at www.pea-journal.eu

Structure, Texture and Tensile Properties of Ti6Al4V Produced by Selective Laser Melting

Radomila Konečná[1], Denisa Medvecká[1], Gianni Nicoletto[2]

[1] Department of Materials Engineering, University of Žilina, Univerzitná 1, 01026 Žilina, Slovak Republic,
e-mail: radomila.konecna@fstroj.uniza.sk
[2] Department of Industrial Engineering, University of Parma, Parco Area delle Scienze 181/A, 43100 Parma, Italy

Article history
Received 05.10.2019
Accepted 23.11.2019
Available online 09.12.2019

Keywords
selective laser melting
Ti6Al4V
powder
structure
tensile test

Abstract
Additive manufacturing has recently expanded its potential with the development of selective laser melting (SLM) of metallic powders. This study investigates the relation between the mechanical properties and the microstructure of Ti6Al4V alloy produced by SLM followed by a hot isostatic pressing (HIP) treatment. HIP treatment minimizes the detrimental influence of material defects. Tensile specimens produced with reference to specific building axes were prepared using a Renishaw A250 system. It has been found that the tensile strength and elongation depend on specimen building direction. Microstructural and textural characterizations were carried out to identify the source of differences.

DOI: 10.30657/pea.2019.25.12 JEL: L69, M11

1. Introduction

Additive manufacturing has recently expanded its potential with the integration in the processing apparatus of high-power highly focused energy source, such as a laser. One technology is denominated selective laser melting (SLM) and is capable of melting and micro welding metallic powders of different composition (Kruth, 2007).

The working principle is based on the iteration of three steps: i) a thin layer of powder resting on a substrate platform is selectively melted to give the desired geometrical cross-section of the part; ii) the building platform is lowered by the typical layer thickness (i.e. 50 μm) and iii) a spreading and levelling system distributes a new layer of powder (Levy, 2010).

The process is repeated until the desired part is layer-wise built. Fig. 1 shows a scheme of an SLM system with the powder shown as grey and the part being built in black. The building chamber is equipped with a low pressure inert gas atmosphere to avoid metal oxygen reaction.

Any 3D part geometry can be obtained directly. Further advantage is saving material and reducing energy consumption when compared to traditional processing techniques. SLM is currently capable of producing near fully dense parts made of high performance materials such as titanium, Ni-based super alloys and stainless steels. SLM is increasingly applied in the aerospace and biomedical sectors (Hollander, 2006; Kahlen, 2001; Rehme, 2005).

However, the relative novelty and the complexity of the processing/microstructure and properties relationships make SLM a manufacturing technology requiring further study (Facchini, 2009; Thijs, 2010; Vracken, 2001).

This study investigates the influence of a SLM process followed by a hot isostatic pressing (HIP) treatment on the structure, texture and mechanical properties of Ti6Al4V alloy specimens.

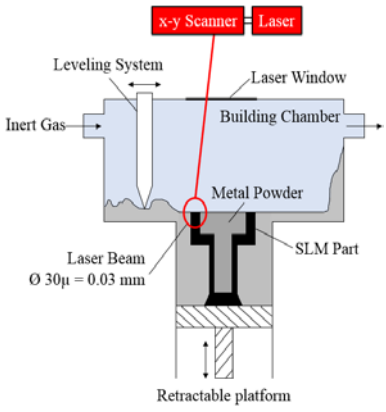

Fig. 1. Scheme of a SLM system

2. Experimental

The material used in this study was Ti6Al4V alloy with chemical composition in the table 1. The spherical Ti6Al4V powder with the controlled granulometry in the range 15 - 45 µm, Fig. 2, was used.

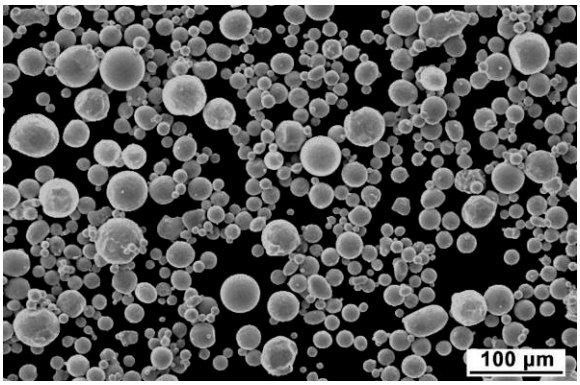

Fig. 2. TiAl64V powder, SEM

Table 1. Chemical composition of the Ti6Al4V powder

Element [wt. %]	Al	V	Fe	O
Standard	5.5 ÷ 6.5	3.5 ÷ 4.5	<0.3	<0.2
Determined elements	6.08	3.9	0.025	0.065
Element [wt. %]	**C**	**N**	**H**	**Ti**
Standard	<0.08	<0.05	<0.015	Bal.
Determined elements	0.007	0.006	0.002	Bal.

The SLM system used in this study was a Renishaw A250 system which uses an ytterbium fibre laser with a wavelength of 1075 nm. The maximum build volume is 245 mm × 245 mm × 300 mm (x, y, z), the build rate 5 cm³ to 20 cm³ per hour, the layer thickness 20 µm to 100 µm, laser beam diameter 70 µm at powder surface and laser power of 200 W.

HIP of the SLM part can be performed to increase its quality and density (Mashl, 2015). The HIPed specimens under investigation were heated to temperature 920 °C and subjected to pressure 1 000 bar for 2 hours in argon. The objective is the closure of all existing discontinuities associated to the layer-by-layer fabrication process.

A characterization of the inherent texture and microstructure of the SLM and HIPed material due to the layer-by-layer selective laser melting process was determined by light microscope (LM) Neophot 32 and SEM Tescan LYRA 3 XMU FEG/SEM with EDX analyser.

Specimens (6.25 x 4 mm² in minimum cross-section) for tensile tests were produced according two orientations with respect to the build direction as shown in Fig. 3 to analyse the influence of fabrication orientation on the structure and mechanical properties.

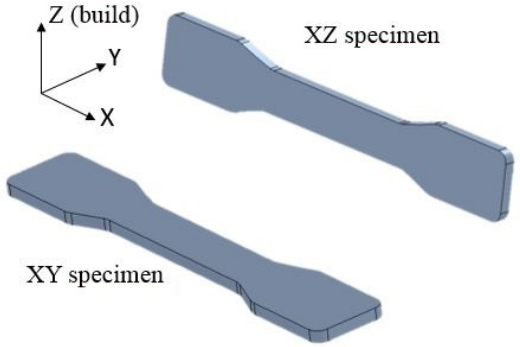

Fig. 3. Specimen orientation with respect to build direction

The main difference between the two specimens is the number of laser melted layers involved. Tensile tests were performed according to ASTM 8/E 8M – 08, using a MTS 810 servo hydraulic machine equipped with a 25 mm-gage length MTS extensometer. The tests were conducted in displacement-control mode (rate 0.01 mm/s). The fractographic analysis of fracture surfaces after tensile test was performed on the Tescan SEM.

3. Results and discussion

3.1. Structure characterization

One specimen with x-z orientation (T2) and one specimen with x-y orientation (T3) shown in Fig. 3 were chosen for metallographic analysis. Metallographic sections were prepared according to transverse and longitudinal directions of the specimens.

The studied Ti6Al4V alloy is a typical two phase α+β structure containing α and β phases which are stabilized by alloying elements, Fig. 4. α phase is stabilized by aluminum, Fig. 4a, b and β phase is stabilized by vanadium, Fig. 4a, c. The HIP process improved porosity and density of the specimens and affected the structure obtained during SLM fabrication phase. The porosity of both specimens is very low and only very small (i.e. several µm in size) defects were identified near the top surface. They could be readily removed by machining. Typical pores observed near the top surface are shown in Fig. 5a. These defects were orientated parallel to the laser scanning direction. In both specimen high roughness was found near the top surface, especially in specimen T3 with x-y orientation, Fig. 6a, b.

The microstructure consists of a lamellar structure of α+β *phases shown in Fig. 5c and Fig. 6c, respectively***.** During the SLM process α´ martensite is formed. The subsequent HIP process converted the original structure into a lamellar α+β structure (Lütjering, 1998; Kubiak, 1998).

The structure of α+β phases is in the form of colonies where parallel α phase lamellae in the elongated primary β phase grain are created during cooling from the high temperature of the HIP process. In each elongated β grain, new colonies nucleate not only on its boundaries but also on

boundaries of the colonies and exhibit the typical Widmanstätten microstructure (1), Fig. 5c, d.

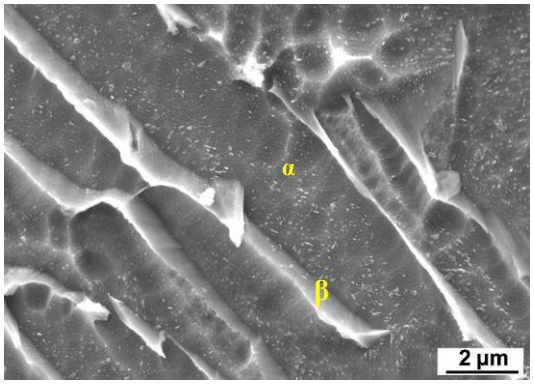

a) details of α and β phases

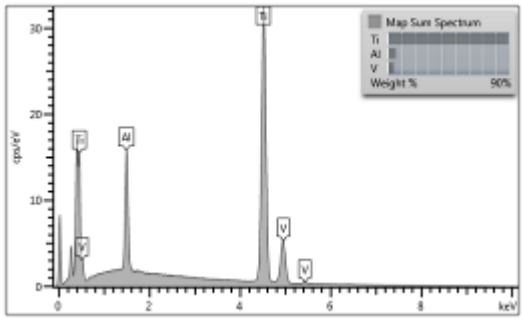

b) high content of Al

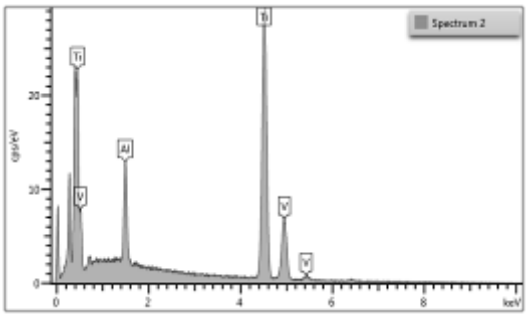

c) high content of V

Fig. 4. EDX point analysis of α and β lamellas

Some of elongated β grains show a coarsening of α phase lamellae (2). The structure analysis revealed in the T3 specimen regions with coarser grains or small equiaxed grains of α phase, Fig. 6c which was better visible in the SEM, Fig. 6d. The higher content of areas with (fine or coarse) α grains may be responsible for lower elongation of T3 compared to T2 specimen. The stabilized α phase increases the strength and decreases the elongation. The thickness of α-lamellae, see for example Fig. 5a and Fig. 6d, and colony size have the most significant influence on mechanical properties (Lütjering, 1998; Gil, 2001; Bača, 2017; Konečná, 2017). Thin lamellas contribute to the higher strength. However, the determination of α colony size is complicated by the presence of the Widmanstätten microstructure, Fig. 5c and Fig. 6c.

3.2. Texture characterization

The macrostructures of specimens are shown in Fig. 5.b and Fig. 6a, b. In the case of specimen T2 (x-z orientation) it is difficult to distinguish a well-defined texture depending on the laser beam scanning direction. The primary β phase grain growth is parallel to the specimen build direction. The build direction for T2 specimen is identified from orientation of light elongated grains and scanning direction is perpendicular to the built up grains orientation. In opposite for specimen T3 the macro view, Fig. 6a, b, shows the texture very well visible and is orientated in the direction of build elongated β grains (Bača, 2016; Konečná, 2016; Konečná, 2017).

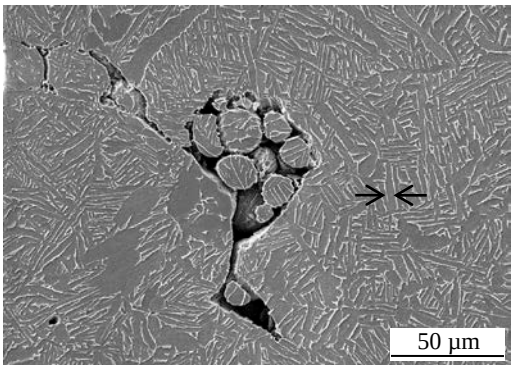

a) typical detail of defect near the top (on the left) of surface α-phase is dark), SEM

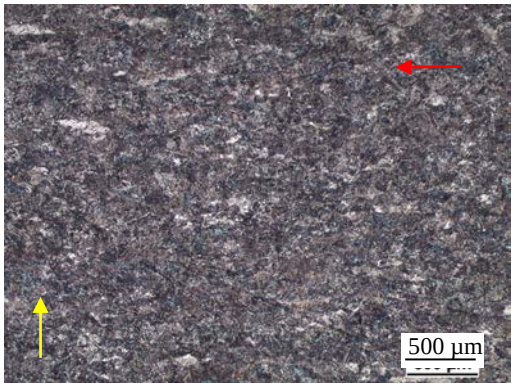

b) red arrow shows build direction, yellow arrow laser scanning direction, LM

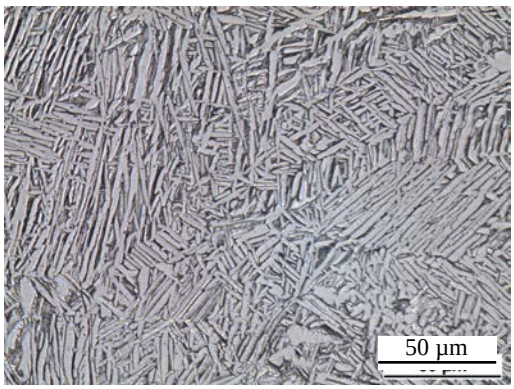

c) lamellar α+β structure (α-phase is light), LM

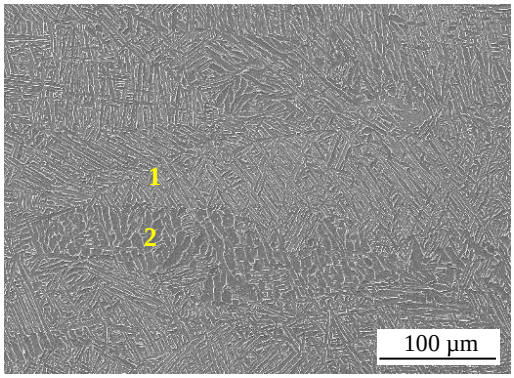

d) different α+β lamellar structure in original elongated β grains, SEM

Fig. 5. Structure of Ti6Al4V, specimen T2, x-z orientation, SLM+HIP, etched 10% HF

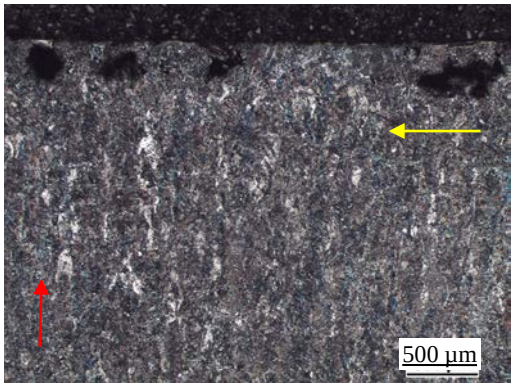

a) transverse section, red arrow shows build direction, yellow arrow laser scanning direction, LM

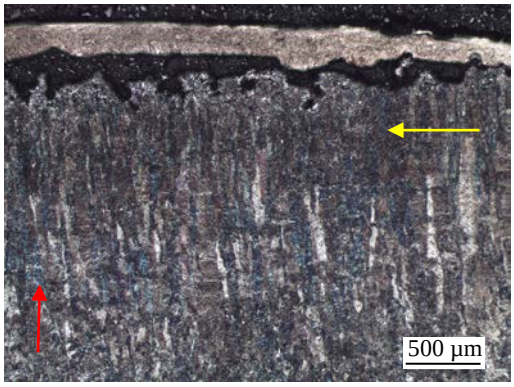

b) longitudinal section – defects on the top surface, LM

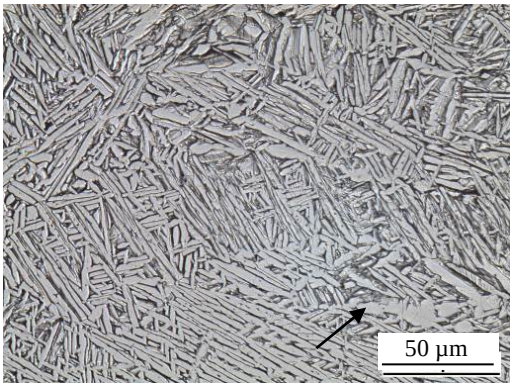

c) lamellar α+β structure (α-phase is light), LM

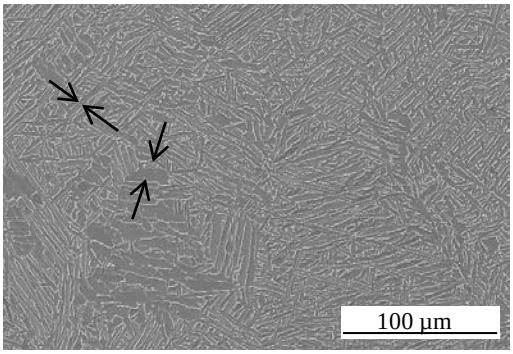

d) region with coarsening grains of α-phase (dark), SEM

Fig. 6. Structure of Ti6Al4V, specimen T3, x-y orientation, SLM+HIP, etched 10% HF

3.3. Tensile testing

Fig. 7 shows the stress-strain responses of the HIPed x-y vs. x-z specimens. They demonstrate consistently a difference in mechanical properties depending on the specimen orientation. The x-y specimens are associated to higher yield stress and ultimate strength (ca. 10 %) and lower elongation to rupture than the x-z specimens. The high temperature exposure of HIP process reduces the ultimate strength R_m of SLM Ti6Al4V from a reference value of about 1300 MPa but significantly improves the elongation to rupture (Thijs, 2010).

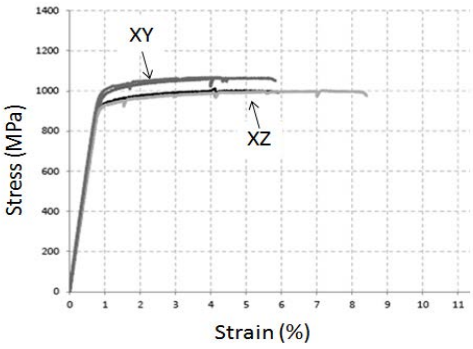

Fig. 7. Stress-strain curves of SLM Ti6Al4V

3.4. Fracture surfaces

Inspection of macro-fracture surfaces after tensile test shows differences between specimens T2 and T3, see Fig. 8a and b. Overview of fracture surface of specimen T2 (x-z) shows higher plastic deformation compared to the specimen T3 (x-y) what is in accordance with measured elongation to rupture shown in Fig. 7.

They both share the same characteristic transcrystalline ductile fracture with dimple morphology but dimples formation and deformation is different. Magnified views of the central region of both fracture surfaces are shown in Fig. 8c and d.

In the case of specimen T2 confirms deep plastically deformed dimples seen in detail in Fig. 8c. The fracture nucleates in the area of α phase nucleation, then plastic flow occurs in the areas of β phase which is much more ductile, close to α phase areas.

Dimple size is typically different for α phase (large) and β phase (small) even if this phase is more plastically deformable than the α phase. The reason is that the β phase is confined between thick α lamellas. The dimples in the region (1) are elongated in the direction of shearing deformation.

The dimple characterizations on the surface of specimen T3 are larger and flat. Initiation of dimple formation was by transcrystalline cleavage visible in Fig. 8d. The reason of the cleavage initiation may depend on the content of large α phase grains, which are brittle compared to the thin β phase.

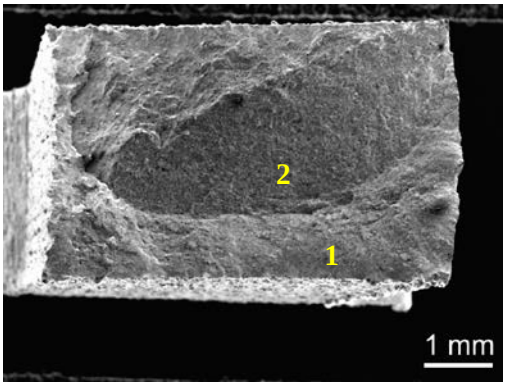

a) overview, specimen T2, x-z orientation, R_m = 950 MPa, A = 7 %

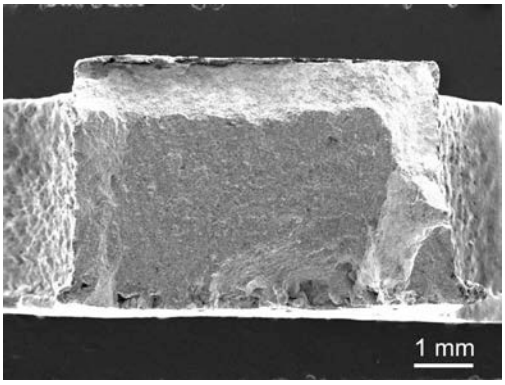

b) overview, specimen T3, x-y orientation, R_m = 1050 MPa, A = 4 %,

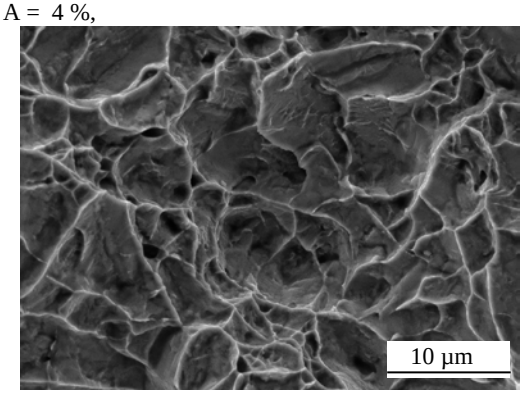

c) dimple morphology, specimen T2, x-z orientation

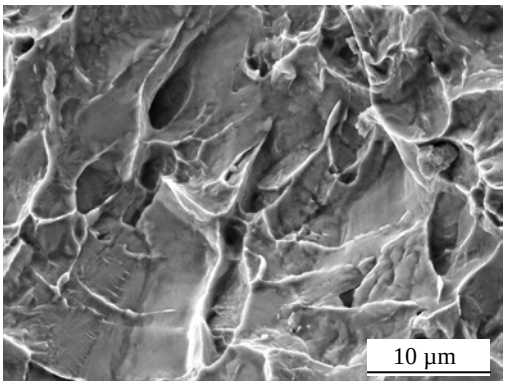

d) large flat dimples, specimen T3, x-y orientation

Fig. 8. Fracture surfaces after tensile test, SEM

4. Summary and conclusion

This study investigated the influence of a SLM process followed HIP treatment on the structure, texture and mechanical properties of Ti6Al4V alloy specimens produced according to different orientations with respect to the specimen build direction. The following conclusions were drawn:

- The HIP treatment applied after SLM preparation results in good material quality and density.
- Higher porosity was observed on the top surface of T3 (x-y) specimen.
- The texture of material produced by SLM technique is not significant after HIP process.
- Both specimen direction buildings result in similar microstructures.
- The x-y orientation building was characterized by higher content of large brittle α phase grains that resulted in higher strength and yield stress and lower elongation when compared to the x-z orientation.
- The dimples on fracture surface of α phase in specimen with x-y orientation are flat and large with originating cleavage crack at their root.

Acknowledgements

This work was supported under the project of Operational Programme Research and Innovation: Research and development activities of the University of Zilina in the Industry of 21st century in the field of materials and nanotechnologies, No. 313011T426. The project is co-funding by European Regional Development Fund.

Part of the research was supported by the project Slovak VEGA grant No. 1/0463/2019. Specimen fabrication by the technological partner BEAM-IT, Fornovo Taro (Italy) is gratefully acknowledged.

Reference

Bača, A., Konečná, R., Nicoletto, G., Kunz, L., 2016. *Influence of Build Direction on the Fatigue Behaviour of Ti6Al4V Alloy Produced by Direct Metal Laser Sintering*. Materials Today: Proceedings, 3(4), 921-924, DOI: 10.1016/j.matpr.2016.03.021.

Bača, A., Konečná, R., Nicoletto, G., 2017. *Influence of the Direct Metal Laser Sintering Process on the Fatigue Behavior of the Ti6Al4V Alloy*. Materials Science, 891, 317-321, DOI: 10.4028/www.scientific.net/MSF.891.317.

Facchini, L., Magalini, E., Pierfrancesco, R., Molinari, A., 2009. *Microstructure and mechanical properties of Ti-6Al-4V produced by electron beam melting of pre-alloyed powders*, Rapid Prototyping Journal, 15(3), 171-178, DOI: 10.1108/13552540910960262.

Gil, F.J., Ginebra, M.P., Manero, J.M., Planell. J.A., 2001. *Formation of alpha-Widmanstatten structure: effects of grain size and cooling rate on the Widmanstatten morphologies and on the mechanical properties in Ti6Al4V alloy*, Journal of Alloys and Compounds, 329 (1-2), 142-152, DOI: doi.org/10.1016/S0925-8388 (01)01571-7.

Hollander, D.A., M. von Walter, M., Wirtz, T., Sellei, R., Schmidt-Rohlfing, B., Paar, O., Erli, H.J., 2006. *Structural, mechanical and in vitro characterization of individually structured Ti-6Al-4V produced by direct laser forming*, Biomaterials, 27(7), 955-63. DOI: 10.1016/j.biomaterials.2005.07.041.

Kahlen, F.J., Kar, A., 2001. *Tensile Strengths for Laser-Fabricated Parts and Similarity Parameters for Rapid Manufacturing*, Journal of Manufacturing Science and Engineering, 123(1), 38-44, DOI: 10.1115/1.1286472.

Konečná, R., Kunz, L., Bača, A., Nicoletto, G. 2016. *Long fatigue crack growth in Ti6Al4V produced by direct metal laser sintering*, Procedia Engineering, 160, 69-76, DOI: 10.1016/j.proeng.2016.08.864.

Konečná, R., Nicoletto, G., Bača, A., Kunz, L., 2017. *Metallographic Characterization and Fatigue Damage Initiation in Ti6Al4V Alloy Produced by Direct Metal Laser Sintering*, Materials Science Forum, 891, 311-316, DOI: 10.4028/www.scientific.net/MSF.891.311.

Konečná, R., Kunz, L., Bača, A., Nicoletto, G., 2017. *Resistance of direct metal laser sintering Ti6Al4V alloy against growth of fatigue cracks.* Eng. Fract. Mechanics, 185, 82-91, DOI: 10.1016/j.engfracmech.2017.03.033.

Kruth, J.P., Levy, G., Klocke, F., Childs, T.H.C., 2007. *Consolidation phenomena in laser and powder- bed based layered manufacturing*, CIRP Annals - Manufacturing Technology, 56(2), 730-759, DOI: 10.1016/j.cirp.2007.10.004.

Kubiak, K., Sieniawski, J., 1998. *Development of the microstructure and fatigue strength of two-phase titanium alloys in the processes of forging and heat treatment*, Journal of Materials Processing Technology, 78(1-3), 117-121, DOI: 10.1016/S0924-0136(97)00472-X.

Levy, G.N., 2010. *The role and future of the Laser Technology in the Additive*. Manufacturing environment, Physics Procedia, 5(A), 65-80, DOI: 10.1016/j.phpro.2010.08.123.

Lütjering, G., 1998. *Influence of processing on microstructure and mechanical properties of (α+β) titanium alloys*, Materials Science and Engineering: A, 243(1-2), 32-45. DOI: 10.1016/S0921-5093(97)00778-8.

Mashl, S.J. 2015. *Powder Metallurgy Processing by Hot Isostatic Pressing*, ASM Handbook, 7, 260-270, DOI: 10.31399/asm.hb.v07.9781627081757.

Rehme, O., Emmelmann, C., 2005. *Reproducibility for properties of selective laser melting products*, Proceedings of the Third International WLT-Conference on Lasers in Manufacturing, Munich, 227-232.

Thijs, L., Verhaeghe, F., Craeghs, T., Van Humbeeck, J., Kruth, J. P. 2010. *A study of the micro structural evolution during selective laser melting of Ti-6Al-4V*, Acta Materialia, 58(9), 3303-3312, DOI: 10.1016/j.actamat.2010.02.004.

Vrancken, B., Thijs, L., Kruth, J. P., Van Humbeeck, J. 2012. *Heat treatment of Ti6Al4V produced by Selective Laser Melting: Microstructure and Mechanical properties*, Journal of Alloys and Compounds, 541(0), 177-185, DOI: 10.1016/j.jallcom. 2012.07.022.

選擇性激光熔煉產生的Ti6Al4V的結構，織構和拉伸性能

關鍵詞
選擇性激光熔化
鈦6Al4V
粉末
結構體
拉伸試驗

摘要
隨著金屬粉末的選擇性激光熔融（SLM）的發展，增材製造最近擴大了其潛力本研究研究了通過SLM進行熱等靜壓（HIP）處理而製備的Ti6Al4V合金的力學性能與顯微組織之間的關係。HIP處理使材料缺陷的有害影響最小化。
使用雷尼紹A250系統準備了參照特定建築軸線生產的拉伸試樣。
已經發現，抗張強度和伸長率取決於樣品構建方向。
進行了微觀結構和紋理表徵以識別差異的來源。